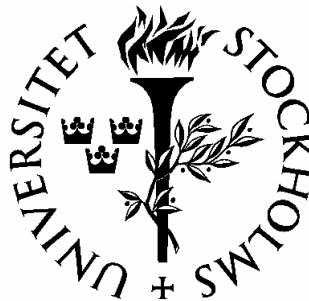


*ConeTrap:
An Electrostatic Ion Trap for
Atomic and Molecular Physics*

AFSHIN FARDI

AKADEMISK AVHANDLING



Department of Physics
Stockholm University
2001

Articles included in this thesis:

- I. A. Fardi, H. Cederquist and H.T. Schmidt (2000): '*Lifetime measurements on metastable He-like ions*' Hyperfine Interactions. **127**, 247.
- II. H. T. Schmidt, H. Cederquist, J. Jensen and A. Fardi (2001): 'ConeTrap: a compact electrostatic ion trap', NIM B **173**, 523.

Articles not included in this thesis:

- III. H.T. Schmidt, S.H. Schwartz, A. Fardi, K. Haghighat, H. Cederquist, L. Liljeby, A. Langereis, J.C. Levin and I.A. Sellin (1998): '*Method for determining absolute partial cross sections for radiative and non-radiative deexcitation of metastable hydrogen-like ions*', Phys. Rev. A, **58**, 2887.
- IV. H.T. Schmidt, S.H. Schwartz, A. Fardi, K. Haghighat, A. Langereis, H. Cederquist, L. Liljeby, J.C. Levin and I.A. Sellin (1999): '*Collisional deexcitation of metastable ions: A new technique to separate radiative and nonradiative contributions*', Proceedings of the XV CAARI, Denton, Texas, 1998, AIP Conf. Proc. **475**, p. 44
- V. A. Sellin, J. C. Levin, H. T. Schmidt, S. H. Schwartz, A. Fardi, K. Haghighat, H. Cederquist, L. Liljeby and A. Langereis (1999) '*Absolute rates for radiative and non-radiative deexcitation of metastable $\text{He}^+(2s)$ in targets of variable polarizability*', NIM B. **154**, 83.
- VI. H. Cederquist, A. Fardi, K. Haghighat, A. Langereis, H. T. Schmidt, S. H. Schwartz, J. C. Levin, I. A. Sellin, H. Lebius, B. Huber, M. O. Larsson, and P. Hvelplund (2000): '*Electronic Response of C_{60} in Slow Collisions with Highly Charged Ions*', Phys. Rev. A **61**, 022712
- VII. S. H. Schwartz, A. Fardi, K. Haghighat, A. Langereis, H. T. Schmidt, and H. Cederquist (2000): '*Absolute and total electron electron-capture cross sections in slow $\text{Ar}^{q+}\text{-C}_{60}$ collisions*', Phys. Rev. A **63**, 013201.
- VIII. A. Langereis, J. Jensen, A. Fardi, K. Haghighat, H. T. Schmidt, S. H. Schwartz, and H. Cederquist: '*Stabilization of electrons on Ar^{q+} after slow collisions with C_{60}* ', Phys. Rev. A **63**, 062725 (2001)

Table of Contents

<i>Abstract</i>	4
1. Introduction	5
2. Design and ion-optics simulations.....	6
3. Experimental tests of ConeTrap.....	9
3.1. The first test with 4 keV Ar^+	9
3.2. Further testing of the ConeTrap with N^+	12
3.2.1. Effects of ion-ion collisions	13
3.2.2. Two storage modes.....	15
3.2.3. Pressure variations	17
4. Planned experiments with ConeTrap.....	20
4.1. Measurement of the lifetime of the metastable negative helium ion using ConeTrapII	21
4.2. Lifetime measurements for the metastable $1s2s\ ^3S$ state in two-electron systems.....	23
4.3. Determination of lifetimes of C_{60}^{q+} , ($q= 2, \dots, 8$).....	25
5. Conclusions	26
<i>References</i>	30
<i>Acknowledgments</i>	32

Abstract

The present work is concerned with the design, construction and successful operation of a very simple, fully electrostatic compact ion trap, ConeTrap. It is demonstrated that ion storage can indeed be obtained and that long storage times are found even at modest vacuum conditions (a lifetime exceeding 100 *ms* is found for 4 *keV* Ar^+ ions at a 10^{-8} *Torr* –range vacuum). Furthermore, two qualitatively different storage modes depending on the detailed trap electrode settings are investigated. It is concluded that the trap is well-suited for lifetime determination experiments. Three such experiments, all of which are under preparation, are briefly described.

1. Introduction

In traditional ion traps the ions are confined either by a combination of electric and magnetic fields, as in a Penning trap [1], or by a time-varying electric field as in a Paul trap [2]. In these devices one can achieve stable equilibrium for a charged particle at rest in the center of the trap. It is, however, not necessary to keep the charged particles at rest in order to confine them. In heavy-ion storage rings the ion beams are exposed to confining forces for parts of the revolution times only. When the Heidelberg Test Storage Ring (TSR) [3], the Aarhus STorage RIng, Denmark (ASTRID) [4], and the CRYRING in Stockholm [5] were designed and constructed in the late 1980's, larger accelerator-rings at e.g. CERN were sources of inspiration. As a consequence, these facilities with their circumferences of 40-55 *m* are still often referred to as 'the small European storage rings'. A large step towards smaller size was recently taken in Århus, when the fully electrostatic storage ring ELISA [6] with a circumference of about 7 *m* was put into operation. At the Weizmann Institute in Israel an even smaller electrostatic storage device was developed consisting of two focusing electrostatic mirrors, each of which is built of eight electrodes to form a proper equipotential surface [7]. Apparently independent of the efforts in Israel, a very similar device applied in mass spectrometry of biomolecules was constructed at the Lawrence Berkeley National Laboratory [8].

We have developed a more compact and simpler electrostatic trap intended mainly for lifetime measurements [9]. The length of the first prototype is 17 *cm* and it consists of only three electrodes. The two identical end electrodes are conical in shape and the center electrode is cylindrical. The working principle is quite simple: Each end electrode, in combination with the center electrode, forms a focusing electrostatic mirror when the end electrode potential is sufficiently high to make the ions turn around. By fine-tuning all three potentials, settings are found where the ions are confined to closed orbits and can be stored for times limited only by the background gas pressure. The trap

is loaded with an externally produced ion beam by lowering the potential of the entrance electrode for a short time. The stored ions can then be extracted at a later time by lowering the voltage of the exit electrode. In the next chapter the trap design is discussed along with the ion optics simulations. Chapter three is the most central part of this work, where the results of the experimental tests are given. Three planned experiment with ConeTrap are discussed, in chapter four before the conclusions, which are given in chapter five.

2. Design and ion-optics simulations

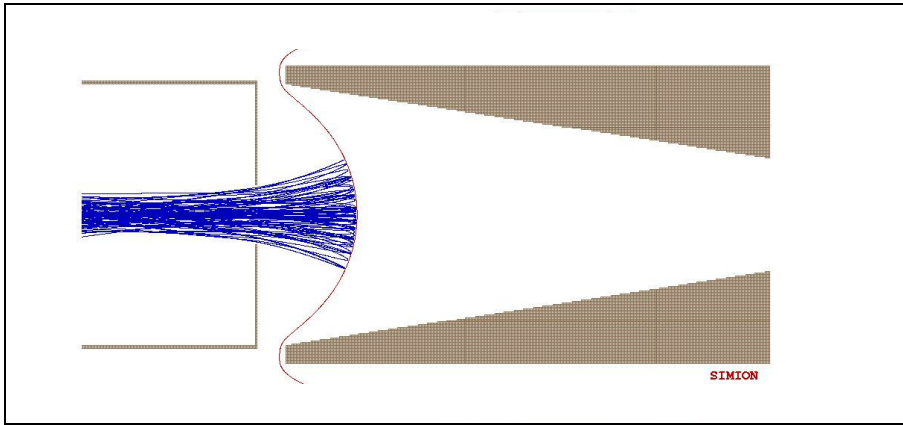


Fig 1. *One focusing electrostatic mirror. The ions are reflected and focused by the curved equipotential surface corresponding to their total mechanical energy*

The electrostatic trap **ConeTrap** consists of two conical electrodes acting as focusing electrostatic mirrors (Figure 1) to keep the fast ions confined for many reflections. The conical geometry makes the equipotential surfaces curve to form a reflecting surface similar to a spherical optical mirror. By proper choice of the dimensions and the applied voltages the focal lengths may be adjusted to make the ion trajectories form stable orbits. Fast ions that are trapped inside, will be reflected back and forth many times until they are extracted or take part in a collision process in which their charge and (or) momentum is changed so that they can no longer be contained. To optimize

the design the ion-optical properties were calculated by means of the ion-optics simulation program SIMION [10].

SIMION solves the Laplace equation for a given electrode and potential configuration and traces ions with pre-defined initial positions and momenta through the electrode configuration. An example of potential surface plots during acceptance, confinement and extraction of an ion pulse is shown in Figure 2. The height of the electrodes is equivalent to the voltage they are connected to. It was found in the simulations that with a proper choice of

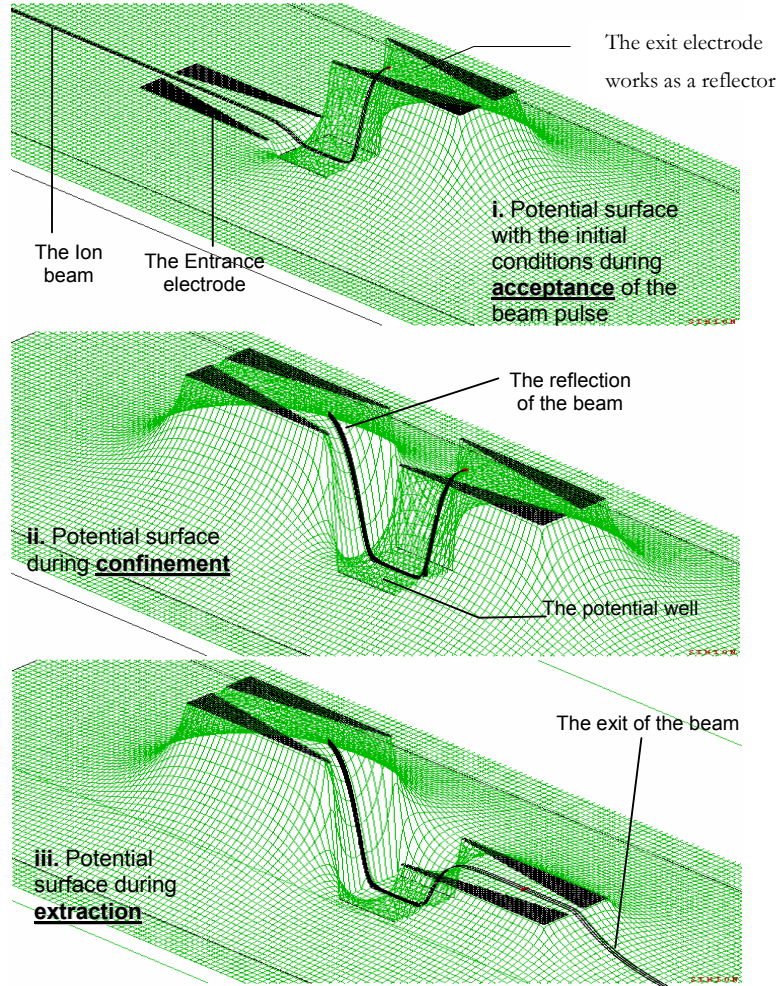


Fig 2. *The potential surface plot*

potentials for the three electrodes during the three phases, true confinement can be achieved. That means that in the simulation the particles can be confined indefinitely.

In Figure 3 we show the design of the trap. The total length of the trap is only 175 mm. The two conical electrodes are 66 mm long and the central electrode is 35 mm long. The entrance and exit apertures are 14.0 mm in diameter and the apertures of the middle electrode are 8.0 mm in diameter. The whole trap is mounted as one unit and it is possible to fine-tune the position of the system relative to the surrounding vacuum chamber to optimize the operation.

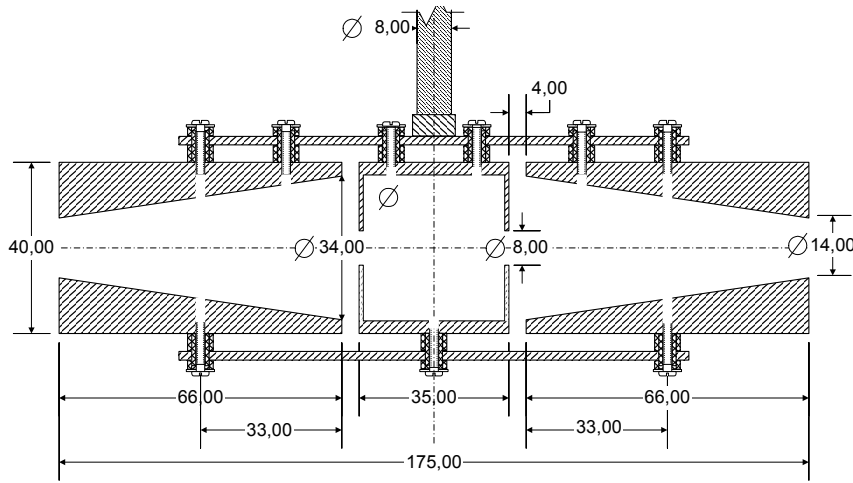


Fig. 3 Design of the ConeTrap (all dimensions in mm)

The trap is loaded with an externally produced ion beam by lowering the potential of the entrance electrode for a short time. The stored ions can then be extracted at a later time by lowering the voltage of the exit electrode. Ions are injected into and extracted from the trap by rapidly changing the potentials of the end electrodes. This is done by means of a number of fast transistor switches (MOSFET) which are described in detail in *Appendix A*.

3. Experimental tests of ConeTrap.

In the following subsections a series of tests of the electrostatic trap is presented. The crucial point is obviously to demonstrate that the device is capable of storing ions for extended periods of time. The role of ion-ion collisions is discussed and we test whether the assumption that residual-gas collisions are the main reason of loss of ions out of the trap is valid. The two qualitatively different storage modes with different ion-trajectories and average storage lifetimes are analyzed.

3.1. The first test with 4 keV Ar⁺

The setup for this test is shown in figure 4. Singly charged argon ions are produced in a gas discharge ion source and transported to the trap at 4 keV, using the electrostatic deflectors and lenses in the ion path between the ion source and the trap. By switching the voltage of one of the deflector plates near the ion source between 0 V and -300 V the beam is chopped. The pulse width is 8 ms and the repetition rate is 1.0 Hz. The trap entrance electrode is switched simultaneously from 4.2 keV to 0 V allowing the ions to enter. The middle and exit electrodes are kept at constant voltages of 200 V and 4.2 keV, respectively. In this ‘open trap’ configuration the ions are reflected from the exit electrode and leave the trap again through the entrance electrode. After 8 ms the entrance electrode is switched back to 4.2 keV with a rise time of less than 30 ns and ions travelling inside the open cone of the exit electrode at this moment will be caught and reflected back and forth between the cone electrodes at a frequency of about 300 kHz. When as is the case in this example, the entrance and exit electrodes are at the same potential, we will refer to that common value as V_{trap} .

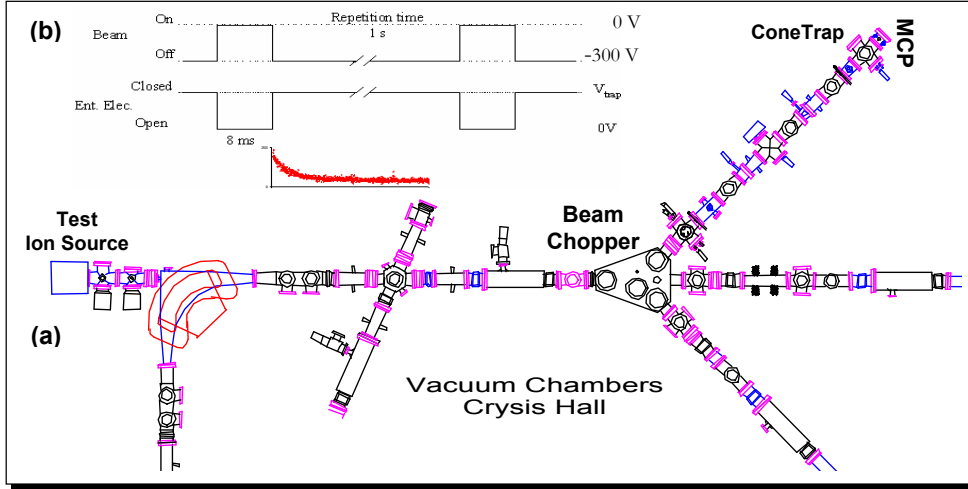


Fig 4. The beam line used in the experiment (a), and timing schematic of the fast voltage switches (b)

The ions in the trap may capture an electron from the residual gas, which in this test was measured to be $7 \cdot 10^{-8}$ mbar N_2 equivalent. A fraction of the neutralized ions will leave the trap through the exit electrode and may be detected by a micro-channel-plate (MCP) detector.

Figure 5 shows the count rate of neutrals on the detector as a function of time after closure of the trap entrance. Simultaneously with the closure of the entrance, the beam chopper switches off the incoming beam (figure 4.b). The detection of neutral particles on the detector after the time when the trap entrance is closed and the incoming beam is switched off, is our evidence that ions are in fact stored in the trap. We have thus demonstrated that ion confinement can be achieved in this fully electrostatic compact ion trap, which to the best of our knowledge is the simplest ion-storage device available.

Assuming that residual gas collisions are the main loss mechanism in the trap, the number of stored ions, N , will follow this rate equation:

$$dN = -N \cdot \langle \mathbf{v} \cdot \boldsymbol{\sigma} \rangle \cdot \frac{P}{k \cdot T} \cdot dt \quad (1)$$

Where v is the speed of the particles, σ is the cross-section for electron capture, P is the pressure, k is Boltzmann's constant and T is the temperature. As v is not constant and the cross-section in general is a function of v we have to introduce the average rate coefficient $\langle v \cdot \sigma \rangle$. We rewrite equation (1):

$$\frac{dN}{dt} = -\frac{N}{\tau} \quad (2)$$

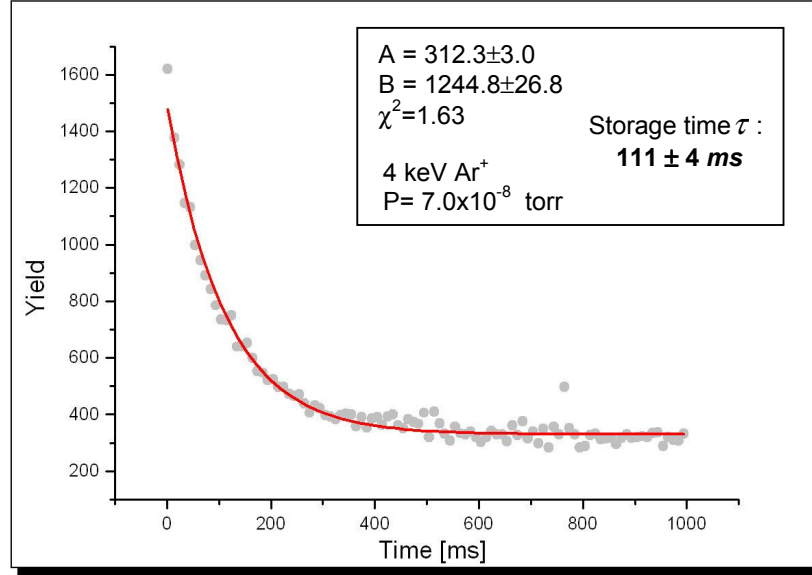


Fig 5. Count rate of neutral atoms leaving the trap as a function of time after injection

Where τ is the **storage lifetime** (τ^{-1} is the decay rate due to residual gas collisions):

$$\tau = \frac{k \cdot T}{P} \cdot \frac{1}{\langle v \cdot \sigma \rangle} \quad (3)$$

The solution to the differential equation (2) is an exponential decay:

$$N(t) = N_0 \cdot e^{-t/\tau} \quad (4)$$

Where N_0 is the number of particles at time $t=0$ s.

The observed count rate will be given by the sum of the actual number of neutral particles hitting the detector and the detector's rate of dark counts. The former is proportional to the number of trapped particles given by equations 4 whereas the latter is constant. The assumption of residual-gas collisions dominating the particle loss has thus led us to expect the count rate to be given by the sum of an exponential function and a constant. To extract the storage lifetime from the data we make a fit to a trial function given by:

$$F(t) = A + B \cdot e^{-t/\tau} \quad (5)$$

To fit a function we use the Least Squares Fit method with χ^2 as a goodness-of-fit parameter. The error of the number of counts in each channel is estimated by \sqrt{Yield} . In the Least Squares Fit the points are weighted according to:

$$w = \frac{1}{error^2} = \frac{1}{Yield} \quad (6)$$

The result of the fit to the data is that the storage lifetime of Ar^+ at the present beam energy and background pressure is 111 ± 4 ms. This time corresponds to more than 60 000 reflections inside the trap before neutralization.

3.2. Further testing of the ConeTrap with N^+

In order to reveal different properties of the ConeTrap further experiments were done. Singly charged atomic nitrogen ions produced in the ion source, are injected into the trap with an energy of 1.4 keV. The experimental setup is presented in figure 6. The reason for choosing atomic nitrogen instead of argon is the following:

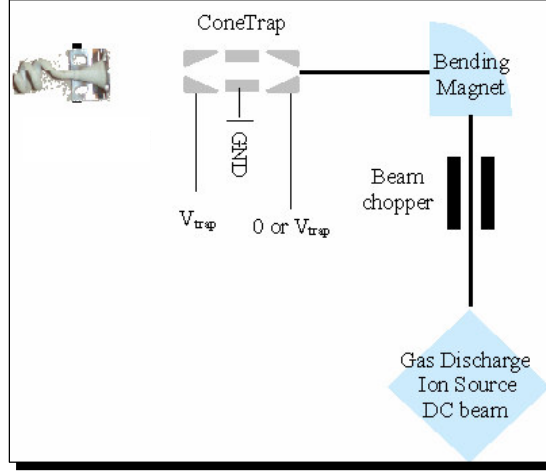


Fig 6. The experiment setup for singly charged atomic nitrogen (N^+)

Due to shortage of differential pumping in this setup (only two pumps, before and after the magnet), the background gas is dominated by the gas flow from the ion source. At the relatively low collision velocities considered here, electron capture is strongly enhanced when the process is exactly resonant as $Ar^+ + Ar \rightarrow Ar + Ar^+$. By using an *atomic* ion (N^+) from a *molecular* precursor (N_2) this effect is avoided and the storage life time is strongly increased.

3.2.1. Effects of ion-ion collisions

Figure 7 shows the neutral yield as a function of time for singly charged atomic nitrogen ions with 1.4 keV energy, a constant background level has been subtracted and the yield plotted on a logarithmic scale. We observe a non-exponential behavior during the first 20 ms . This is especially so when higher currents are injected, $I_{\text{ion}} > 3 \text{ nA}$. The observation of non-exponential behavior and particularly its intensity dependence calls for improved analysis.

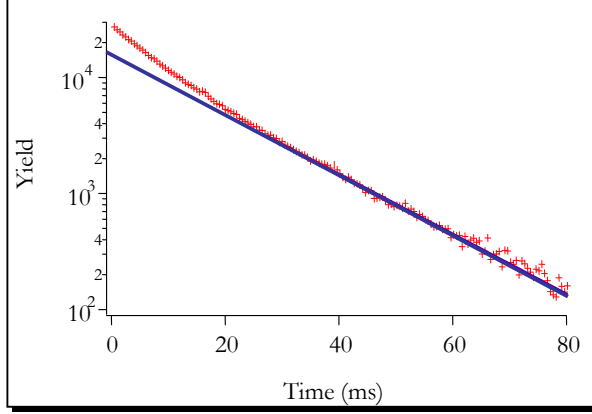


Fig 7. *The observed decay compared to a single exponential*

We assume that the faster decay is caused by interionic interactions and add a loss term proportional to the square of the number of ions to the rate equation (Eq. 2), which now reads:

$$\frac{dN}{dt} = -\frac{N}{\tau} - \gamma \cdot N^2 \quad (5)$$

where the parameter γ depends on the detailed geometry and the ion-ion scattering cross-section. The analytical solution to this equation is:

$$N(t) = \frac{1}{\left(\frac{1}{N_0} + \gamma \cdot \tau \right) \cdot e^{t/\tau} - \gamma \cdot \tau} \quad (6)$$

where N_0 is the initial number of ions, and τ now represents the lifetime found in the long-time limit where the ion-ion interaction can be neglected. Using equation (6) and making a new fit to our data we get a much better agreement as demonstrated in figure 8. Based on this observation we conclude that the observed deviation from an exponential decay is caused by ion-ion collisions.

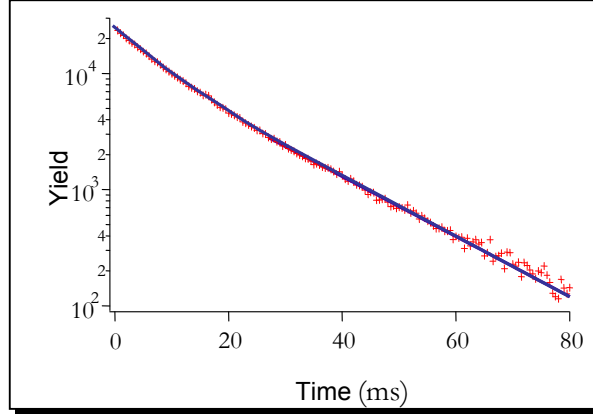


Fig 8. *The new fit with ion-ion effect taking to account*

3.2.2. Two storage modes

One of the most intriguing features of ConeTrap is that it has two qualitatively different storage modes. During the N^+ experiment we varied the trapping potential (we refer to the common value of the voltages of the exit and entrance electrodes after the entrance closure as the trapping potential or V_{trap}) and recorded the number of neutrals on the detector in the time interval $200\ \mu s$ to $700\ \mu s$ after injection. This is a measure of the ion capture capability at the particular voltage. We concluded that there exist two regions of trapping potential where ions can be confined: **One is a narrow range just above the acceleration voltage** ($1.4\ kV$ in this particular case) **and the other is a wider range at higher voltage between $1.9\ kV$ and $2.3\ kV$.** Figure 9 clearly shows that the capture capability is at its maximum around $1.450\ kV$ and it decreases rapidly so that around $1.5\ kV$ there is no confinement at all. Then the number of stored ions increases from $1.8\ kV$ with a maximum around $2.1\ kV$ and goes down to zero at $2.4\ kV$.

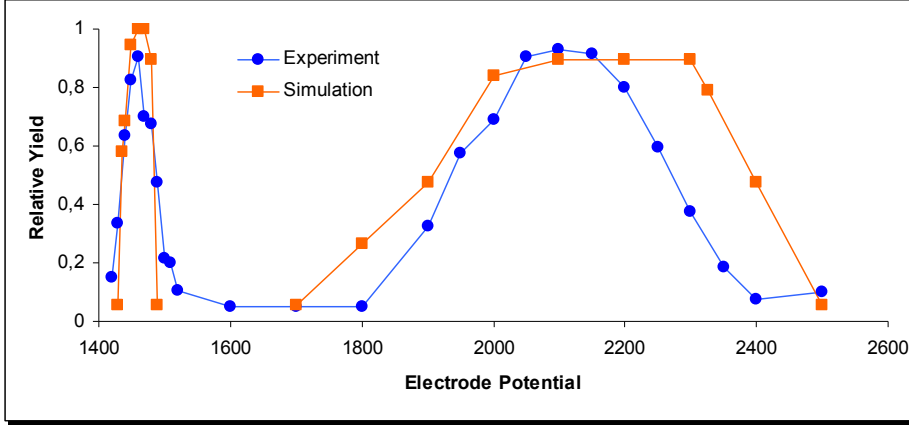


Fig 9. Measured trapping of 1.4 keV N^+ for different V_{trap} both in simulations and experiment

Also shown in figure 9 are the results of ion-optic simulations. A beam with a high emittance is represented by a large number of ion-trajectories with slightly varying initial conditions. The Relative Yield is determined as the function of the ion trajectories that lead to stable orbits at the given value of V_{trap} . We find a good agreement between experiment and simulation. An important difference between these two modes is that the ion storage lifetimes are significantly different. Figure 10 (a) and (b) below reveals that the storage lifetime in the lower region is longer than the storage time in the higher region

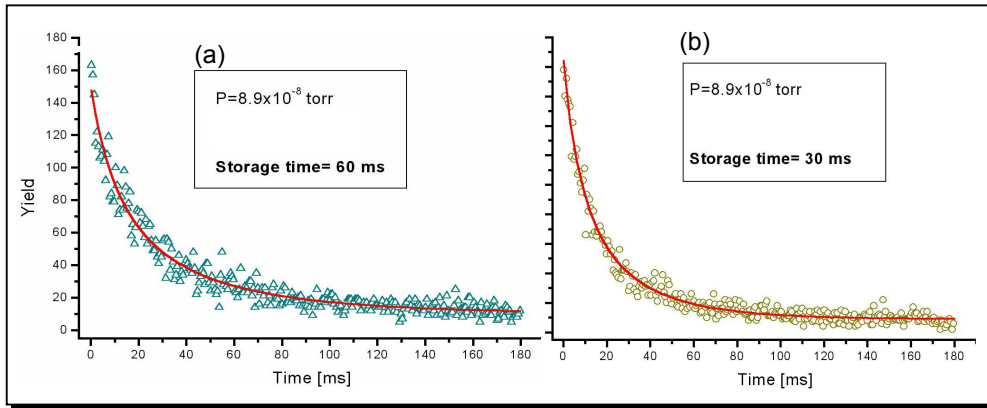


Fig 10. Lifetime measurements for 1.4 keV N^+ in the two trapping regions (a) Lower region, (b) higher region

($\tau_{\text{low}} = 60 \text{ ms}$, $\tau_{\text{high}} = 30 \text{ ms}$). We shall return to this problem with a more elaborate analysis in the next section.

As shown in figure 9, the observed pattern of confinement –no confinement as a function of the trapping potential (Figure 9) was reproduced in the ion trajectory simulations. These simulations also revealed what the ion trajectories look like in the different cases: **In the lower voltage range** (figure 11-a) **they are smoothly bent** whereas in the higher voltage region (figure 11-b) **the ions are reflected by the limiting equipotential surface like photons by a curved mirror.**

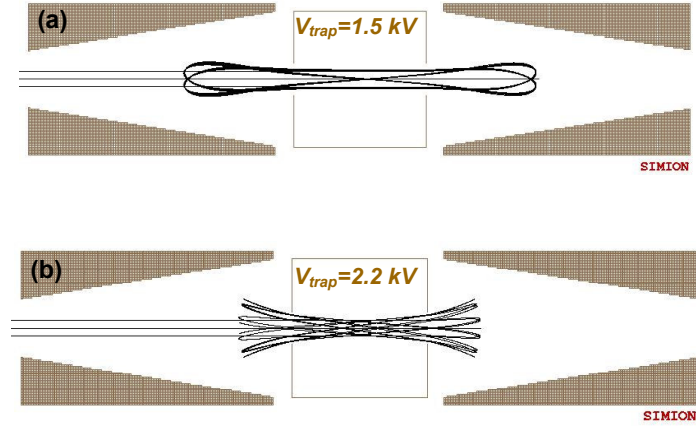


Fig 11. SIMION simulations for different values of the trap potential V_{trap} defined in the text

3.2.3. Pressure variations

In the experimental setup in figure 6 the easiest way to vary the pressure was to increase the gas flow into the ion source. This leads to increase of the molecular nitrogen gas in the trap area. The lifetime measurements were performed at different pressures ranging from $4 \cdot 10^{-6} \text{ Torr}$ to $9 \cdot 10^{-8} \text{ Torr}$. We observe the pressure dependence shown in figure 12 and table 1.

PRESSURE [Torr]	STORAGE TIME [ms]	
	<i>Mode 1</i>	<i>Mode 2</i>
4.8×10^{-6}	2.7 ± 0.05	1.47 ± 0.03
2.2×10^{-6}	5.6 ± 0.52	3.30 ± 0.13
4.5×10^{-7}	22.7 ± 0.80	10.4 ± 0.73
8.9×10^{-8}	57.9 ± 4.1	36.1 ± 3.10

Table 1. *The measured pressure dependence in both modes*

These tests confirmed that background gas collisions are the dominant loss mechanism and suggest that storage lifetimes exceeding one minute may be achieved if UHV conditions are introduced.

From equation (3) we derive:

$$\frac{1}{\tau} = \frac{\langle \mathbf{v} \cdot \boldsymbol{\sigma} \rangle}{kT} \cdot P \quad (7)$$

That means the storage lifetime τ is inverse proportional with the pressure P with proportionality constant:

$$\alpha = \frac{\langle \mathbf{v} \cdot \boldsymbol{\sigma} \rangle}{kT} \quad (8)$$

In figure 12 we show the pressure dependence of the trapped ions in both modes. We could derive the proportionality constants α_1 and α_2 from figure 12 for *mode 1* and *mode 2* which are the slopes of the linear fits.

$$\left. \begin{array}{l} \alpha_1 = 0.0079 \pm 0.00001 \\ \alpha_2 = 0.0142 \pm 0.00045 \end{array} \right\} \frac{\alpha_1}{\alpha_2} = 0.56 \pm 0.06 \quad (9)$$

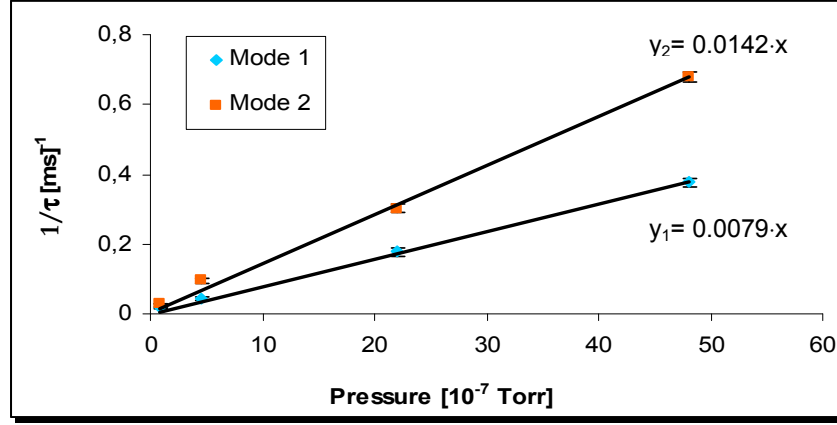


Fig 12. The pressure variation in both modes.

As the temperature is constant Equation (8) implies that:

$$\frac{\langle \mathbf{v} \cdot \boldsymbol{\sigma} \rangle_1}{\langle \mathbf{v} \cdot \boldsymbol{\sigma} \rangle_2} = \frac{\alpha_1}{\alpha_2} \quad (10)$$

At this low collision velocity the non-resonant electron capture cross-section is only expected to have a weak velocity dependence. We may thus expect the ratio of the average rate coefficients to be given by the ratio of the average speeds and thus:

$$\frac{\langle \mathbf{v} \rangle_1}{\langle \mathbf{v} \rangle_2} = \frac{\alpha_1}{\alpha_2} \quad (11)$$

We derive the average velocities from the ion-optic simulations. If the time for one turn around of a particle stored in the trap is t and the distance between the turning points l , the mean velocity of a particle bouncing back and forth between the outer electrodes is:

$$\langle \mathbf{v} \rangle_1 = \frac{2 \cdot l_1}{t_1} \text{ and } \langle \mathbf{v} \rangle_2 = \frac{2 \cdot l_2}{t_2} \quad (12)$$

where the subscripts (1 and 2) stand for *mode 1* and *mode 2*. The numerical values for l and t are obtained from the simulations for both modes.

$$\left. \begin{array}{l} l_1 = 47 \text{ mm} \\ t_1 = 2.2 \mu\text{s} \end{array} \right\} v_1 = 42.8 \text{ km/s} \quad \text{and} \quad \left. \begin{array}{l} l_2 = 29 \text{ mm} \\ t_2 = 0.8 \mu\text{s} \end{array} \right\} v_2 = 72.4 \text{ km/s} \quad (13)$$

The ratio between v_1 and v_2 could be written as:

$$\frac{v_1}{v_2} = 0.59 \Rightarrow \frac{v_1}{v_2} \approx \frac{\alpha_1}{\alpha_2} \quad (14)$$

This agrees with the found ratio $\frac{\alpha_1}{\alpha_2}$. This means that the different lifetimes found in the two modes is explained by the different average speeds and thus the average *distance* traveled before the neutralization in a residual gas collision is the same in the two modes.

4. Planned experiments with ConeTrap

Several interesting experiments are possible using the **ConeTrap** presented here or slightly modified versions of it. A few examples are: Lifetime measurements of metastable positive and negative ions, preparation of vibrationally cold beams for molecular ion experiments inside or after the trap, laser experiments with positive and negative atomic and molecular ions. Here we describe three lifetime measurements, which all have been granted beam time at the Manne Siegbahn Laboratory by the Crying Program Advisory Committee (CPAC). The lifetimes to be determined are those of He^+ ($1s2s2p^4P$), Mg^{10+} ($1s2s^3S$) and C_{60}^{q+} for $2 \leq q \leq 10$.

4.1. Measurement of the lifetime of the metastable negative helium ion using ConeTrapII

If we consider the He atom in the metastable state of $1s2s\ ^3S$ and its interaction with a third electron we find that the $1s2s2p\ ^4P$ state of He^- is bound by $77\ meV$ with respect to the parent neutral state. This state can decay by autodetachment to the He ground state and a free electron, but since the spin is not conserved in this decay, the rate is strongly suppressed. Two of the fine-structure components ($J=1/2$ and $J=3/2$) are coupled to the rapidly autodetaching resonance state $1s2s2p\ ^2P$ by the spin-orbit coupling and have lifetimes of the order of $10\ \mu s$, whereas the $J=5/2$ level has a lifetime of about $350\ \mu s$.

Only two experimental results with better than 10 % accuracy are available for the lifetime of the $J=5/2$ level: At the Århus storage ring ASTRID the result $350 \pm 15\ \mu s$ was achieved [11]. Two systematic effects limited the accuracy of this measurement. The magnetic fields mixed the $J=5/2$ level with the nearby shorter-lived $J=3/2$ level and the Black Body Radiation from the room temperature vacuum chamber walls was found to photodetach the He^- ions with sufficient efficiency to severely affect the results. Recently this situation was improved in a measurement using an electrostatic storage device developed at the Weizmann Institute in Israel. Due to the absence of magnetic fields, one of the above mentioned sources of error was eliminated and the slightly more accurate result $343 \pm 10\ \mu s$ was achieved [12].

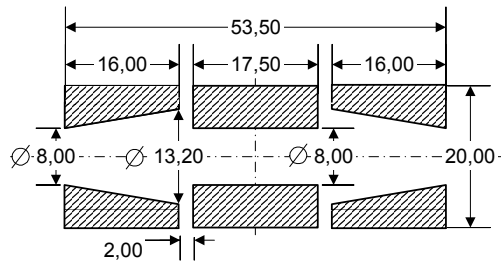


Fig 13. Design of ConeTrapII (all dimensions in mm)

We plan to measure the lifetime of the He^- ion in the smaller version of **ConeTrap** shown in figure 13 cooled to liquid nitrogen temperature in order to suppress the effect of black body radiation induced photo detachment. The negative ions are produced in charge exchange in a Calcium (Ca) vapor cell and injected into the cold trap where they move with keV kinetic energy between the two electrostatic mirrors. Neutral He atoms produced in the decay of the negative ions may exit and be detected by a Ceratron electron multiplier detector. The rate of neutrals as a function of the time after injection yields the decay curve from which the characteristic lifetime is deduced.

The technique described here is not limited to the He anion, other negative systems can be considered as well. Efforts to measure the He^- lifetime in a cold environment are also made at the Weizmann Institute [12] and in Århus where the electrostatic storage ring ELISA is applied in these studies. While writing this thesis an article was published by Pedersen et al. [17] which disclosed a lifetime of $365 \pm 3 \mu s$, which is 6% longer than the lifetime reported by Wolf et al. [12]. That result [17] was obtained by cooling the electrostatic storage ring to $-50^\circ C$.

ConeTrapII, is approximately 1/3 of the original ConeTrap making it relatively easy to cool to liquid nitrogen temperature. The new trap is placed inside a closed copper box together with an electrostatic parallel plate energy analyzer in front and a ceratron behind the trap. The entire box is cooled by contact with a liquid nitrogen cooled copper plate. The purpose of the parallel plate analyzer is to bend the ion beam 90° before it enters the ConeTrap to make sure that the ions stored inside the trap cannot ‘see’ the warm vacuum chamber walls outside of the box through the 4 *mm* aperture for beam injection.

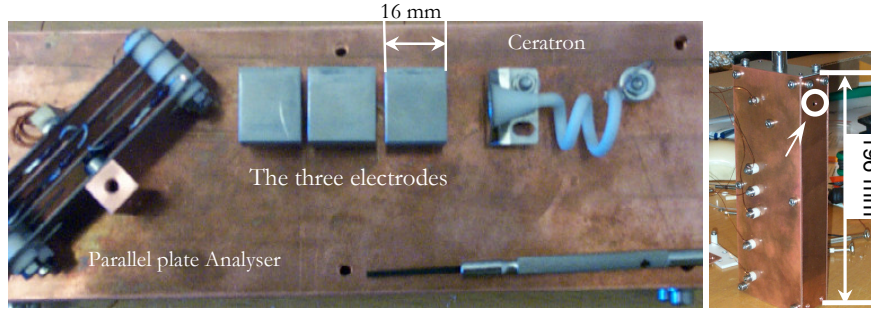


Fig 14. A look inside the 19.6 cm long copper box containing the parallel plate analyzer, the compact ConeTrapII and the ceratron electron multiplier particle detector

We have tested the new trap by storing He^+ ions. The result of the recent very

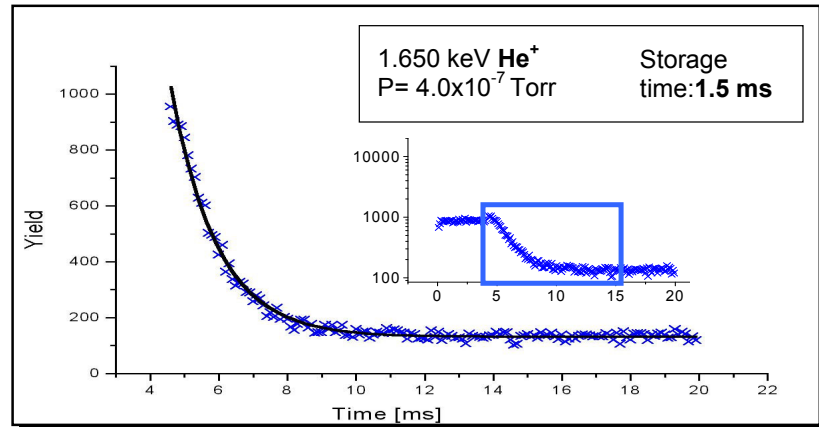


Fig 15. Count rate of neutral He-atoms leaving the trap as a function of time after injection

first test of ConeTrapII is shown in figure 15. We successfully confined (1.65 keV) He^+ ions in the trap with a storage lifetime of about 1.5 ms at a background pressure of $4.0 \cdot 10^{-7}$ Torr.

4.2. Lifetime measurements for the metastable $1s2s^3S$ state in two-electron systems

The first excited state in a He-like ion is the metastable $1s2s^3S$ state, the dominating decay mode of which is a forbidden magnetic dipole transition to the ground state. Until 1993 no experimental methods were available to extract

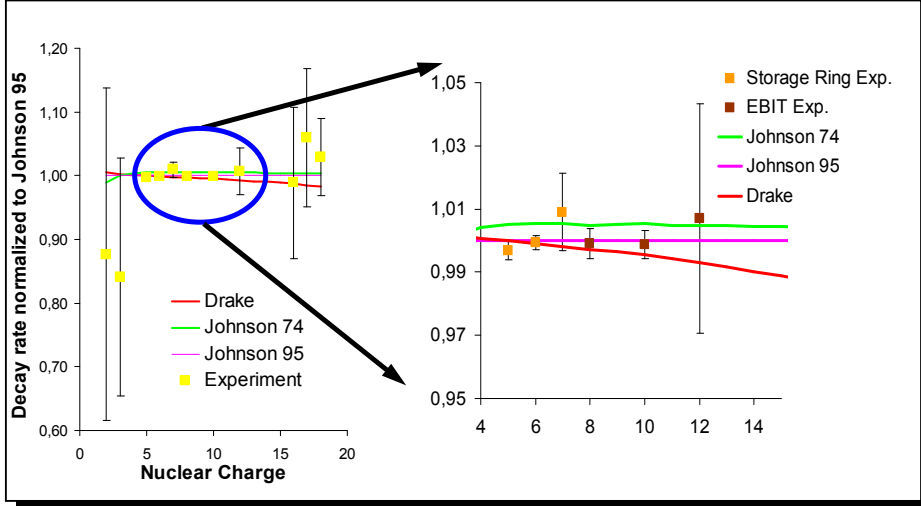


Fig 16. *Theoretical results in comparison with experiments*

lifetimes of this state for nuclear charges in the range $3 < Z < 16$ corresponding to micro- and milli-second lifetimes. In recent years this situation has dramatically improved with several measurements with better than one per cent accuracy. The EBIT group at the Lawrence Livermore National Laboratories have made lifetime determinations in the μs range [13] and in the ms range measurements were made at the TSR storage ring in Heidelberg [14]. The present status of the comparison between experiment and theory for this problem is that all the observations agree with the results of a non-relativistic calculation by Drake emphasizing the electron correlation aspect [15], but also with a more recent relativistic calculation [16]. In figure 16 the experimental and the theoretical results for the M1-decay rate relative to the most modern theoretical result are shown as a function of the nuclear charge. To distinguish between the two theoretical results sub-per cent accuracy measurements are needed in the range of nuclear charges between 10 and 15.

The ion beams (first Ne^{8+} and later Mg^{10+}) for this experiment are provided by the new high-intensity Electron Cyclotron Resonance (ECR) ion source at the Manne Siegbahn Laboratory. A beam from the ECR source will be injected directly into the ConeTrap and the emitted x-ray will be observed by means of

a channeltron detector, which has an efficiency of about 10% for the present wavelength which is 9.3 Å . A rough estimate of the number of ions in the trap, the solid angle of the detector and the detection efficiency gives an expected count rate of 0.1-1 x-ray photon per injection. By pulsing the trap entrance electrode at the maximum frequency of 10 kHz the statistical error will become very small even for short measuring times.

4.3. Determination of lifetimes of C_{60}^{q+} , ($q= 2, \dots, 8$)

Three of the articles on the publication list, but not included in the thesis, concern collisions between highly charged ions and C_{60} . The latest development in this project is that we now extract the intact C_{60} ions and charged fragments and identify them by means of a time-of-flight mass spectrometer. A time-of-flight spectrum from a recent experiment with Xe^{30+} projectiles is shown in figure 17. We are interested in determining how highly charged intact C_{60}^{q+} ions can be stable on the μs time scale set by the experiment. The next step will be to inject multiply charged C_{60}^{q+} ions in a ConeTrap to determine the lifetime for different charge states. The ConeTrap will be integrated in a new time-of-flight spectrometer. This way the desired charge state can be selected by opening the trap entrance briefly at the appropriate time.

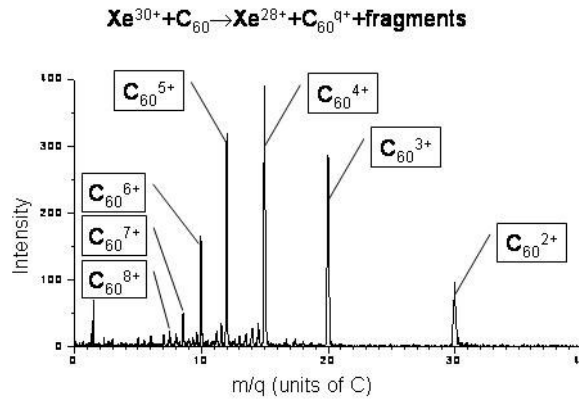


Fig 17. The mass spectrum of intact C_{60} ions

5. Conclusions

The main conclusion of the present work is that storage of ions in the simple ConeTrap can be achieved. Two different storage modes are identified and further it is shown that for modest intensities the loss of ions out of the trap is dominated by residual gas collisions. ConeTrap is well suited for lifetime measurements and three such proposed experiments are discussed briefly.

Appendix A

To be able to operate the ConeTrap i.e. the trapping and releasing of the ions in a controlled manner, one needs to change the voltages on different electrodes rapidly. A switch accomplishes this voltage changes. Some important parameters should be kept in mind while designing this device. The voltage that needs to be switched which has directly to do with the ion beam energy, rise and fall time which should be short enough that it does not affect the ion beam path in any way in our case calculated to be in μs -region.

The main component of the switching device is a HTS-41-06-GSM which is a high voltage, high current, fast transistor switch. It switches up to 4kV and 60A. The rise time of the switch is highly dependent on the total capacitive load of the system that is to be switched. In our case the rise time has been measured (with a voltage probe, 1:1000) to be less 50 μs .

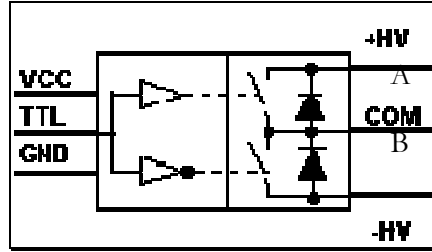


Fig 17. *The internal module schematic of the HTS-41-06-GSM*

These series of switching modules consist of two identical MOSFET switching paths that form a so called push-pull circuit. Both switching paths are controlled by a common driver, which also provides a logic signal negation for one of the switches. The push-pull principle is considered to be especially advantageous in our application because of the capacitive load.

The switches are controlled by positive signals of 3 to 10 volts amplitude. Fault conditions such as over frequency, thermal overload and incorrect auxiliary

supply, set the switching path **A** in off-state and switching path **B** in on-state. Faults are also indicated by a TTL-signal at the fault signal output. It is worth to notice that when the 5VDC supply is not connected, both paths (**A** and **B**) are in off-state. This means that without 5VDC the output potential is undefined, if high voltage is still applied.

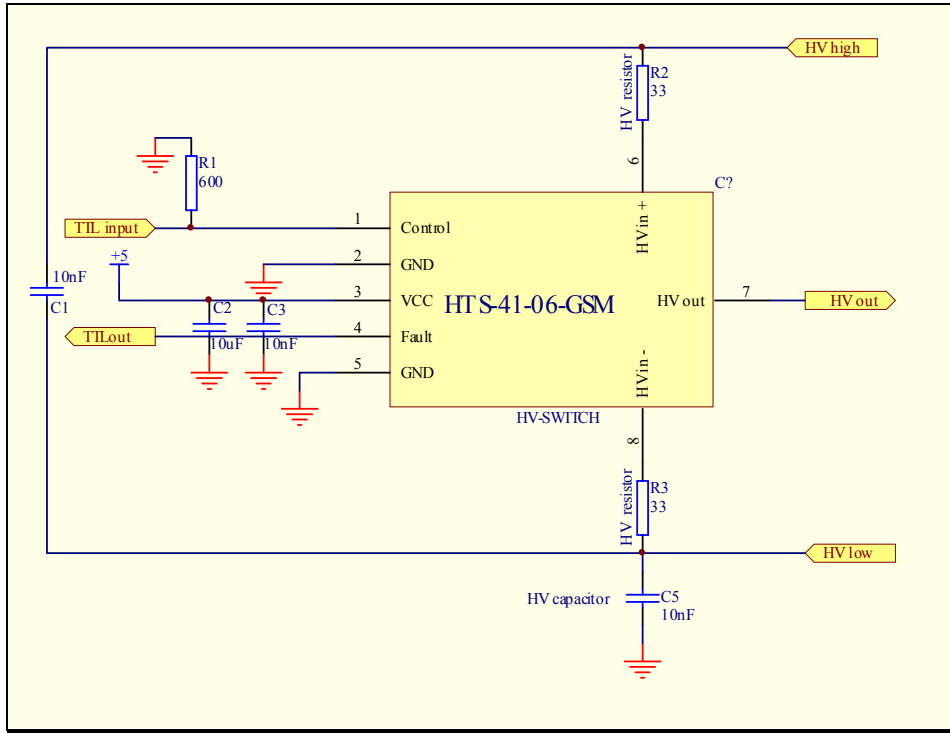


Fig 19. Schematic of one of the switching modules, consisting of the commercial switching unit and surrounding components designed by the author

Technical specification

Specification	Value and Unit
Maximum Operating Voltage	4 kVDC
Typical Breakdown Voltage	8 kVDC
Galvanic Isolation	20 kVDC
Minimum Output Pulse Width	150 μ s
Maximum Output Pulse Width	No Limitation
Minimum Pulse spacing (switch recovery time)	400 ns
Max. Continuous Switching Frequency	12 kHz
Rise & Fall Time	≥ 6 ns
Auxiliary Supply Voltage ($\pm 5\%$)	5 VDC
Auxiliary Supply Current	500 mA

Table 2. Technical specification for the *HTS-41-06-GSM*

References

- [1] L. S. Brown and G. Gabrielse (1986), Rev. Mod. Phys. **58**, 233
- [2] W. Paul and M. Raether (1955), Z. Phys. **140**, 262
- [3] D. Habs *et al.* (1989), Nucl. Instr. and Meth. in Phys. Res. B **43**, 370.
- [4] S. P. Møller (1993), Proc. of the 1993 Particle Accelerator Conf., Washington DC. Edited by S. T. Corneliussen, p. 1741
- [5] K. Abrahamsson et al. (1993) Nucl. Instr. and Meth. in Phys. Res. B **79**, 269
- [6] S. P. Møller (1997), Nucl. Instr. and Meth. in Phys. Res. A **394**, 281.
- [7] D. Zajfman, O. Heber, L. Vejby-Christensen, I. Ben-Itzhak, M. Rappaport, R. Fishman, M. Dahan (1997) Phys. Rev. A **55**, R1577.
- [8] W. Henry Benner (1997), Analytical Chemistry, Vol. 69, No. **20**, 4162.
- [9] H. T. Schmidt, H. Cederquist, J. Jensen and A. Fardi (2001): ‘*ConeTrap: a compact electrostatic ion trap*’, NIM B **173**, 523.
- [10] D. A. Dahl, SIMION 3D, version 6.0, User’s Manual distributed by Ion Source Software, P.O. Box 2776, Idaho Falls, ID 83403, USA.
- [11] T. Andersen, L. H. Andersen, P. Balling, H. K. Haugen, P. Hvelplund, W. W. Smith, and K. Taulbjerg, Phys. Rev. A (1993) **47**, 890.
- [12] A. Wolf, K. G. Bushan, I. Ben-Itzhak, N. Alstein, D. Zajfman, O. Heber, and M. L. Rappaport, Phys. Rev. A (1999) **59**, 267.
- [13] E. Träbert *et al.*, Phys. Rev. A (1999) **60**, 2034.
- [14] H. T. Schmidt et al. Phys. Rev. Lett. (1994) **72**, 1616.
- [15] G. W. F. Drake, Phys. Rev. A (1971) **3**, 908.
- [16] W. R. Johnson et al. Adv. At. Mol. Opt. Phys. (1995) **35**, 255.

- [17] U. V. Pedersen, M. Hyde, S. P. Möller, and T. Andersen, Phys. Rev. A (2001) **64**, 012503.

Acknowledgments

The author wishes to express sincere appreciation to Docent H. T. Schmidt, without whose support, guidance and money this work would not be achievable.

In addition, special thanks to Professor M. Larsson and Professor H. Cederquist for their economical support of this project.

Thanks also to the members of the Atomic Physics and the Molecular Physics group and Dr. J. Jensen from the Manne Siegbahn Laboratory for their valuable input.